

Characterization of Ferredoxin:Thioredoxin Reductase Modified by Site-directed Mutagenesis*

Dominique A. Glauser‡§, Florence Bourquin‡¶, Wanda Manieri||, and Peter Schürmann**

From the Laboratoire de Biochimie végétale, Université de Neuchâtel, CH-2007 Neuchâtel, Switzerland

Ferredoxin:thioredoxin reductase (FTR) is a key regulatory enzyme of oxygenic photosynthetic cells involved in the reductive regulation of important target enzymes. It catalyzes the two-electron reduction of the disulfide of thioredoxins with electrons from ferredoxin involving a 4Fe-4S cluster and an adjacent active-site disulfide. We replaced Cys-57, Cys-87, and His-86 in the active site of *Synechocystis* FTR by site-directed mutagenesis and studied the properties of the mutated proteins. Mutation of either of the active-site cysteines yields inactive enzymes, which have different spectral properties, indicating a reduced Fe-S cluster when the inaccessible Cys-87 is replaced and an oxidized cluster when the accessible Cys-57 is replaced. The oxidized cluster in the latter mutant can be reversibly reduced with dithionite showing that it is functional. The C57S mutant is a very stable protein, whereas the C87A mutant is more labile because of the missing interaction with the cluster. The replacement of His-86 greatly reduces its catalytic activity supporting the proposal that His-86 increases the nucleophilicity of the neighboring cysteine. Ferredoxin forms non-covalent complexes with wild type (WT) and mutant FTRs, which are stable except with the C87A mutant. WT and mutant FTRs form stable covalent heteroduplexes with active-site modified thioredoxins. In particular, heteroduplexes formed with WT FTR represent interesting one-electron-reduced reaction intermediates, which can be split by reduction of the Fe-S cluster. Heteroduplexes form non-covalent complexes with ferredoxin demonstrating the ability of FTR to simultaneously dock thioredoxin and ferredoxin, which is in accord with the proposed reaction mechanism and the structural analyses.

Ferredoxin:thioredoxin reductase (FTR)¹ is the central enzyme of the ferredoxin/thioredoxin system, a redox regulatory

* This work was supported by Grants 31-56761.99 and 3100-067934.02 from the Schweizerischer Nationalfonds. The costs of publication of this article were defrayed in part by the payment of page charges. This article must therefore be hereby marked "advertisement" in accordance with 18 U.S.C. Section 1734 solely to indicate this fact.

‡ Both authors contributed equally to this work.

§ Present address: Fondation pour Recherches Médicales, CH-1211 Genève, Switzerland.

¶ Present address: Paul Scherrer Institut, CH-5232 Villigen, Switzerland.

|| Present address: College of Pharmacy, Medical Center, University of Cincinnati, Cincinnati, OH 45267-0004.

** To whom correspondence should be addressed: Laboratoire de Biochimie végétale, Université de Neuchâtel, Rue Emile-Argand 11, CH-2007 Neuchâtel, Switzerland. Tel.: 41-32-718-2206; Fax: 41-32-718-2201; E-mail: peter.schurmann@unine.ch.

¹ The abbreviations used are: FTR, ferredoxin:thioredoxin reductase; Trx, thioredoxin; FNR, ferredoxin:NADP reductase; DTT, dithiothreitol; FPLC, fast protein liquid chromatography; WT, wild type.

mechanism, which enables oxygenic photosynthetic cells to switch between light and dark metabolism and to adapt to changes in light intensity (1, 2). It transfers a redox signal received from ferredoxin to thioredoxins (Trxs) by a unique mechanism involving a 4Fe-4S cluster and a disulfide bridge, thereby transforming the signal from an "electron signal" to a "thiol signal." Trxs, the regulatory disulfide proteins, transmit this signal by dithiol-disulfide interchange reactions to certain enzymes, e.g. chloroplast fructose-1,6-bisphosphatase (3) and NADP-dependent malate dehydrogenase (4), thereby modifying their catalytic activity through reduction of regulatory disulfide bonds. Most biochemical investigations have been done on the spinach enzyme, whereas the only three-dimensional structure was solved for the *Synechocystis* FTR (5). This enzyme shows no functional difference to the spinach protein but is significantly more stable (6, 7).

The FTR is an unusually thin molecule in the shape of a concave disk with only 10 Å across the center of the molecule where the Fe-S cluster and the redox-active disulfide are located (8). It contains seven strictly conserved cysteine residues, six of them organized in two CPC and one CHC motifs. These six Cys constitute the redox-active disulfide bridge and ligate, in an unusual arrangement, the Fe-S cluster (9). In the *Synechocystis* FTR Cys-57 and Cys-87 form the active-site disulfide. The four remaining cysteines, Cys-55, Cys-74, Cys-76, and Cys-85, are ligands to the cluster. This arrangement positions the redox-active disulfide bridge adjacent to the cluster with Cys-57 exposed to the solvent on one side of the flat molecule, whereas Cys-87 is protected. The iron-sulfur center is closer to the opposite side of the thin molecule. It has been proposed that the two sides of the molecule represent, respectively, the ferredoxin and the Trx docking areas, enabling the FTR to interact simultaneously with electron donor and acceptor (8).

Based on spectroscopic measurements and on the structure a two-step reaction mechanism has been proposed for the reduction of Trx by FTR (8, 10). The first electron, delivered by ferredoxin on the ferredoxin docking area and transmitted through the 4Fe-4S, cleaves the active-site disulfide producing a surface-exposed sulfhydryl (Cys-57) and a cysteine-based thiyl radical (Cys-87). This radical becomes stabilized by the covalent attachment of the cysteine to the cluster, forming an oxidized (3+) five-coordinate cluster. Cys-57 then acts as a nucleophile and attacks the disulfide bond of a Trx, forming a one-electron-reduced heterodisulfide intermediate. His-86 and Arg-58, which are very close to the disulfide bridge (3.9 and 5.6 Å, respectively), might increase the nucleophilicity of the cysteine. This first reaction anchors the Trx molecule through the heterodisulfide linkage to the Trx docking area. The ferredoxin docking area, on the opposite side, stays free for a second interaction with a reduced ferredoxin. The second electron reduces the cluster-ligated Cys-87 and reestablishes the original 2+ oxidation state of the cluster. The newly reduced internal

Cys-87 attacks and cleaves the heterodisulfide linkage between FTR and Trx, thus liberating the reduced Trx. The closing of the active-site disulfide bridge completes the reaction cycle.

Alkylation of the accessible cysteine of the active-site disulfide (Cys-57 in *Synechocystis*) with *N*-ethylmaleimide provided a stable analogue of the one-electron-reduced heterodisulfide intermediate (10, 11). This modification is accompanied by a typical change of the visible spectrum (12) because of the oxidation of the cluster from its 2+ state in the resting enzyme to the 3+ state in the analogue of the reaction intermediate. Recent spectroscopic analyses demonstrated that in the reaction intermediate Cys-87 is coordinated to the closest iron atom of the cluster (13). In addition there is partial bonding of the disulfide to this iron even in the resting state of the enzyme. This promotes charge buildup on this special iron making it an electron donor with increased ferrous character. The system is therefore primed and ready to accept an electron from ferredoxin to break the disulfide bond. The binding of an additional cysteine to the special iron, in the one-electron-reduced heterodisulfide intermediate, makes it more ferric, and the charge is drawn away from it. Thus Cys-87 appears to be a critical residue not only as a member of the disulfide bridge but also because it interacts with an iron atom of the cluster in the resting enzyme.

In this study we have produced and characterized mutant FTRs, based on the *Synechocystis* protein, to obtain further information on the function of three important residues. We individually replaced the redox-active cysteines, Cys-57 by serine and Cys-87 by serine or alanine, as well as His-86, proposed to increase the nucleophilicity of the active site, by tyrosine. The choice of tyrosine was based on sequences of putative FTRs in two archaeobacteria (14, 15). Our results confirm the functions attributed to the two active-site cysteines and provide evidence that His-86 indeed increases the reactivity of the FTR. In addition we have used the wild type (WT) as well as the mutant FTRs to study their interaction with ferredoxin and Trxs. We obtained non-covalent complexes with ferredoxin, covalent heterodimeric complexes with Trxs, representing the one-electron-reduced reaction intermediates, and triple complexes involving all three proteins confirming the protein-protein interactions postulated based on the structural analyses.

EXPERIMENTAL PROCEDURES

Materials—Restriction endonucleases were from Promega and Biolabs, and *Taq* and *Pfu* DNA polymerases were from Promega. They were used according to the manufacturers' instructions. The custom oligonucleotides were obtained from Microsynth AG (Balgach, Switzerland). Chromatography supports and FPLC equipment were from Amersham Biosciences. All chemicals were of analytical grade.

Site-directed Mutagenesis—The construction of the mutant proteins was based on the dicistronic construct for the expression of the FTR from *Synechocystis* sp. PCC6803 described earlier (6, 16).

Mutagenesis was performed by PCR. The three mutations C87S, C87A, and H86Y were introduced by directly amplifying the entire expression vector using the following oligonucleotides (mutations in bold): C87S antisense, 5'-AAACAACATAGAGTGACATTC-3'; C87A antisense, 5'-AAACAACATAGCGTGACATTC-3'; H86Y antisense, 5'-AAACAACATACAGTAACATTC-3'; and SUB1 sense, 5'-TTAACCCCA-GATAACGATTTTG-3'. For the introduction of the fourth mutation, C57S, two successive amplifications were necessary as described for the spinach FTR (7). In a first amplification, using the primers C57S antisense, 5'-GTGGCGAGAGGGGCACA-3', and T7 sense, 5'-AATAC-GACTCACTATAG-3', a megaprimer was obtained containing the information for the variable and part of the catalytic subunit including the mutation. In a second amplification using the megaprimer and T7term antisense 5'-GCTAGTTATTGCTCAGCGG-3', the dicistronic construct was rebuilt and could be inserted into the pET-3c expression plasmid. All sequences and mutations were checked by automatic sequencing using either the T7 or T7term primers and the sequencing kit from Amersham Biosciences on a MWG LICOR sequencer.

Protein Expression and Purification—Expression of recombinant proteins was done in *Escherichia coli* cells grown in Luria broth at 37 °C

either in a 1.5-liter (MultiGen, New Brunswick, CT) or 10-liter fermenter (Model L1523, Bioengineering AG), sparged with air, and stirred at 500 rpm.

Spinach fructose-1,6-bisphosphatase and Trx *f* WT as well as the C49S mutant were expressed and purified as described earlier (17). Mutant spinach Trx *m* C40S was constructed based on Trx *m_c* (18) by PCR, and the product was cloned into the expression plasmid pET-3c and expressed in *E. coli* strain BL21(DE3) (19). It was purified to homogeneity as described earlier (20). Recombinant *Synechocystis* ferredoxin was constitutively expressed in *E. coli* cells (strain DH5a from Invitrogen), transformed with the expression vector pCK5/19 (gift from Herbert Böhme, University of Bonn), and grown overnight in the presence of 50 μM FeSO₄ and 100 μg/ml ampicillin. The purification of ferredoxin was achieved through hydrophobic interaction, size exclusion, and anion exchange chromatography. Ferredoxin:NADP reductase (FNR) from spinach leaves has been purified to homogeneity.

WT and mutant *Synechocystis* FTRs were expressed in the *E. coli* strain BL21(DE3)pLysS in the presence of 50 μg/ml ampicillin, 34 μg/ml chloramphenicol, and 10 mM glucose. When the culture reached an A_{600 nm} of 6–7, expression was induced by adding isopropyl-β-D-thiogalactopyranoside to a final concentration of 0.2 mM, and 2 h later cells were harvested by centrifugation (2400 × *g*, 6 min, 4 °C). The purification of the FTR was done as described elsewhere (16).

Analytical Procedures—Spectrophotometry was performed with a PerkinElmer Lambda 16 instrument. Difference spectra were recorded in dual-compartment cuvettes with compartment path lengths of 0.438 cm. Thiol determinations were done according to Habeeb (21). The activity of FTR was measured by its capacity to activate fructose-1,6-bisphosphatase, using dithionite-reduced benzyl viologen as the electron donor for the FTR as described earlier (22). Gel electrophoretic analyses of the heteroduplexes were done under non-denaturing conditions in a Mini-Protean (Bio-Rad) with the buffer system described by Laemmli (23), omitting SDS and 2-mercaptoethanol, however.

Dissociation of the WT FTR-Trx *f* heteroduplex by the thylakoid system was achieved in a 200-μl incubation mixture containing 100 mM Tris-Cl, pH 7.9, 10 mM sodium ascorbate, 0.2 mM 2,6-dichloroindophenol, 10 μM ferredoxin, 40 μM WT FTR-Trx *f* heteroduplex, and spinach thylakoids equivalent to 100 μg of chlorophyll. After equilibration with argon for 5 min in the dark at 25 °C, the mixture was illuminated for 10 min. Thylakoids were removed by centrifugation, and the 50-μl supernatant was separated on a Superdex-75 HR 10/30 column.

Redox titrations were performed by incubating heteroduplexes in mixtures of oxidized and reduced DTT of defined redox potentials (24) followed by analysis of the mixtures by native gel electrophoresis, which separates heteroduplexes from free FTR and Trxs. This experimental approach provided very reproducible results allowing a good estimate of the redox potential. Incubations were done with 50 μM heteroduplex in 300 mM Tris-Cl, pH 7.0, and 100 mM DTT under argon at room temperature. Equilibrium was reached after 2 h when samples, large enough to easily visualize the proteins, were removed and analyzed on 15% native polyacrylamide gels.

Heteroduplex Formation—Small amounts of heteroduplex were obtained by incubating equimolar solutions of FTR and Trx in 20 mM triethanolamine-Cl buffer, pH 7.3, for 2–4 h at room temperature. Larger quantities of heteroduplex were prepared by mixing FTR (up to 2 μmol) and a 1.2–1.5-fold excess of Trx in 20 mM triethanolamine-Cl buffer, pH 7.3, and 100 mM DTT to reduce possible mutant Trx homodimers. The mixture was concentrated to about 5 ml in an Amicon ultrafiltration cell (Model 12) fitted with an YM-10 membrane and diafiltered with 10 volumes of the above buffer without DTT. The diafiltered solution was transferred to a beaker permitting good oxygenation and slowly stirred overnight at 4 °C. Then the heterodimer was separated from free FTR and Trx by ion exchange chromatography on a Q-Sepharose HiLoad column and finally concentrated and diafiltered with 20 mM triethanolamine-Cl buffer, pH 7.3.

RESULTS

Production and Purification—The WT and mutant *Synechocystis* FTRs were well expressed in *E. coli* and could be purified by our standard procedure except for the C87S mutant. This mutant, although produced in *E. coli* as evidenced by immunoblotting, could not be purified. The Cys to Ser mutation apparently generates an unstable protein, whereas the C87A mutation yields a more stable protein. We obtained yields of purified proteins in the range of 7–27 mg/liter of bacterial culture.

Spectral Characterization—WT FTR has a typical UV-visible

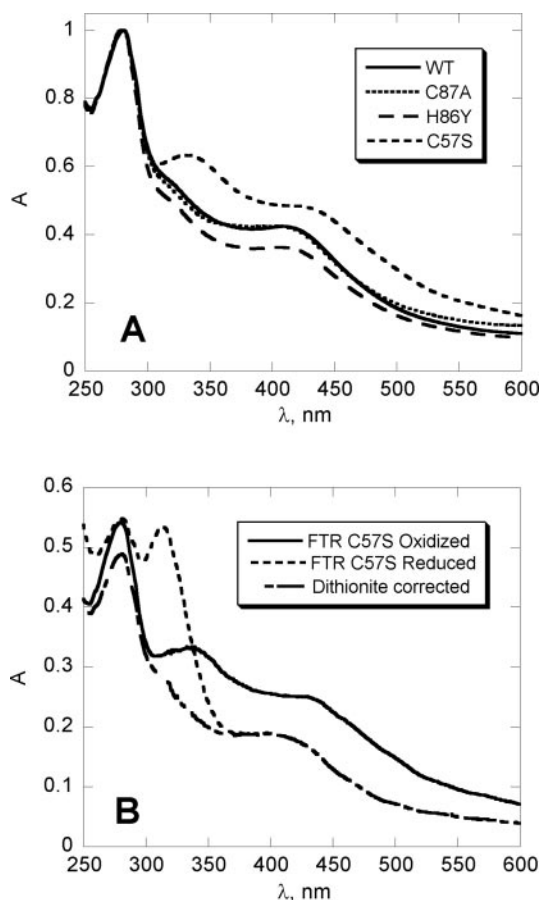


FIG. 1. UV-visible absorbency spectra. *A*, spectra of WT and three mutant FTRs, normalized at 278 nm. *B*, spectra of oxidized and reduced C57S mutant FTR. The peak at 315 nm is caused by excess dithionite. For the dithionite corrected spectrum the absorbency of dithionite has been subtracted.

absorbency spectrum, which is characteristic of the 4Fe-4S cluster in its 2+ redox state and its interactions with the redox-active disulfide bridge (16). Changes in the environment of the Fe-S cluster are therefore expected to influence the spectral properties. Fig. 1A shows the spectra of the WT and the three mutant proteins, and Table I lists their molar absorbencies at 408 nm and the spectral ratios at 408/278 and 408/345 nm calculated from the spectra. The spectra of the mutants C87A and H86Y are very similar to that of the WT protein, except for small differences in the absorbency ratios. In the case of the H86Y mutant the lower 408/278 ratio is explained by the presence of the additional tyrosine. The spectrum of the C57S mutant is clearly different from that of the WT FTR, identical to the one observed with the *N*-ethylmaleimide-modified FTR (11, 12), and appears to be caused by the oxidation of the Fe-S cluster to its 3+ redox state. This has been verified by treating WT and mutant proteins with dithionite. Comparable with what was reported earlier for the WT protein (11), we observed no change in the C87A or H86Y FTR spectra. However, reduction of mutant C57S clearly transforms its spectrum to the type observed with WT FTR as isolated, indicating that the cluster is in the 2+ redox state (Fig. 1B). During oxidation of the added dithionite, because of the presence of oxygen in the cuvette, the spectrum of the C57S mutant shifts back to its original oxidized form.

Changes of the spectra of the four proteins over time were used to compare their stability in solution, an approach already applied successfully to the spinach FTR (7). These results (data not shown) indicate that the C57S mutant has the most stable

conformation. The WT and H86Y mutant are about equally stable but less than the C57S. The C87A mutant is significantly more labile, progressively losing its color during incubation, which indicates that the Fe-S cluster disintegrates.

Thiol Determinations—The accessible and total thiols have been determined by reacting the proteins with 5,5'-dithiobis(2-nitrobenzoic acid) in the absence and presence of SDS to verify the correctness of the mutations and the intactness of the structures. For the WT and the mutants H86Y and C57S the experimentally determined values correspond to the theoretically expected numbers, *i.e.* one accessible and five total thiols in the WT and H86Y FTR, and one accessible and six total thiols in the C57S mutant. For the C87A mutant the expected two accessible thiols were found; however, there were only four instead of six total Cys residues. This might be because of the formation of an artifactual disulfide bond in this less stable mutant under our aerobic assay conditions.

Activity—The catalytic activity of the mutants was measured as their capacity to activate fructose-1,6-bisphosphatase and compared with that of the WT protein. As expected, the two mutations modifying the active-site disulfide, C57S and C87A, completely abolish activity. The mutant H86Y had only ~10% of the WT activity when tested under comparable conditions.

Non-covalent Interaction with Ferredoxin—*Synechocystis* FTR and ferredoxin form a 1:1 complex resulting in a typical difference spectrum with a peak at 460 nm and a trough at 410 nm (Fig. 2A, inset). We titrated the *Synechocystis* FTR mutants with ferredoxin to verify whether the mutations influence this protein-protein interaction. The results show that at a low salt concentration all mutants form a 1:1 complex like the WT protein (Fig. 2A). These complexes are stabilized by electrostatic interactions and have a high affinity, because concentrations above 200 mM NaCl had to be added to observe a deviation from linearity in the formation of the complexes. Curiously, with the mutant C87A the absorbency difference due to the complex started to decrease when ferredoxin above an equimolar ratio was added (Fig. 2B).

Interaction with Thioredoxins through Formation of Covalent Heteroduplexes—Reduction of Trxs proceeds via the formation of a transient, covalent heteroduplex between FTR and Trx. This intermediate complex can be stabilized using mutants in which one or both non-accessible Cys of the participating disulfide bridges are modified. We used mutant Trxs *f* C49S and *m* C40S as well as WT and all three mutant FTRs to study the formation of such heteroduplexes. Their presence could be demonstrated by chromatography and by native gel electrophoresis followed by immunoblotting. SDS-PAGE was not suited for these analyses because of artifactual S-S bond formation upon denaturation under oxidizing conditions leading to multiple bands. When the WT FTR as well as the mutants C87A and H86Y are incubated with Trx *f* C49S a new band appears upon electrophoretic analysis. This band is colored, clearly visible during migration like the band representing FTR, and reacts with antibodies against Trx *f* indicating that it represents the heteroduplex. Similar results were obtained with WT FTR and mutant Trx *m*. When dithiothreitol is added to the electrophoresis samples the heteroduplex band disappears. Upon incubation of the FTRs with WT Trx *f*, no heteroduplex is formed. Also the FTR C57S mutant did not form a heteroduplex, because its interacting Cys had been replaced. We observed, however, that in the presence of Trx *f* C49S, the C57S mutant was degraded. This was verified by following the A_{408}/A_{278} absorbency ratio of an equimolar mixture of the two proteins. Fig. 3A shows that the ratio decreases because of the disintegration of the Fe-S cluster leading to a degradation of the protein, whereas the ratio of FTR incubated alone does not change.

TABLE 1
Spectral properties of WT and mutant FTRs and of FTR-Trx heteroduplexes

FTR	Color	408 nm $M^{-1} cm^{-1}$	Spectral ratio	
			408/278 nm	408/345 nm
WT	Brown-green	17,400	0.44	0.94
C87A	Brown-green	17,400	0.44	1.00
H86Y	Brown-green	17,400	0.41	0.96
C57S	Brown-red	18,700	0.47	0.78
WT-Trx <i>f</i>	Brown-red		0.35	0.78
WT-Trx <i>m</i>	Brown-red		0.30	0.78
C87A-Trx <i>f</i>	Brown-green		0.29	1.00

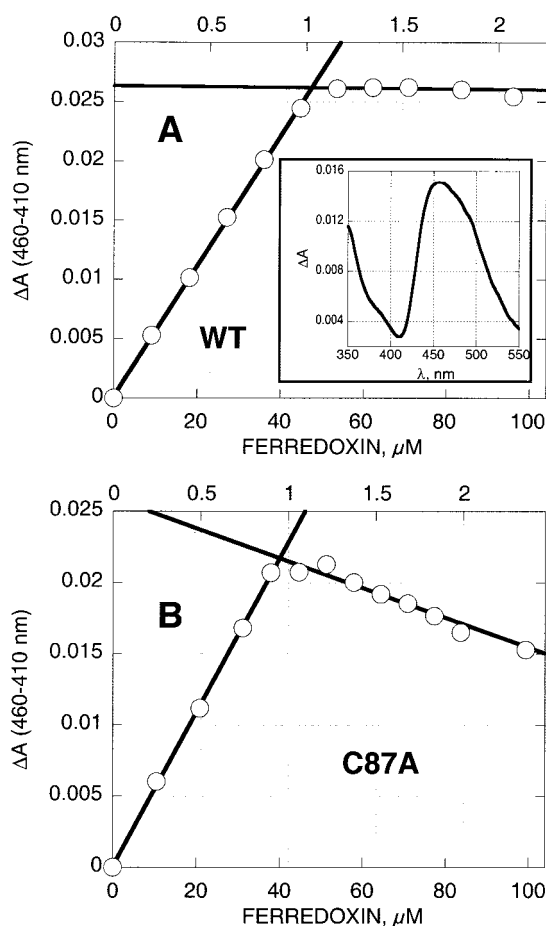


FIG. 2. Complex formation between FTR and ferredoxin. WT (A) and mutant (B) FTR were titrated with ferredoxin in 20 mM triethanolamine-Cl buffer, pH 7.3, at 25 °C. Inset, difference spectrum of the complex FTR-ferredoxin at 23 μM . Difference spectra were recorded using dual compartment cuvettes. To the solution of about 50 μM FTR in the measuring cuvette small aliquots of ferredoxin were added. In the reference cuvette corresponding aliquots of ferredoxin were added to buffer in one compartment and aliquots of buffer to the solution of FTR in the second compartment. After 5 min of equilibration, three spectra from 550 to 350 nm were recorded for each data point, and the difference was calculated from the averaged absorbencies at 460 and 410 nm corrected for dilution. Upper axis represents the ferredoxin/FTR ratio calculated with the exact protein concentrations.

The heteroduplexes were separated from the unreacted proteins by chromatography. Whereas gel filtration did not completely resolve heteroduplex and FTR, because of the relatively small difference in molecular mass, ion exchange chromatography provided quantitative separation of all proteins engaged in the reaction (Fig. 4). This approach enabled us to purify and characterize the heteroduplexes and to use them for interaction studies with ferredoxin.

The visible absorbency spectra of free and Trx-complexed FTR

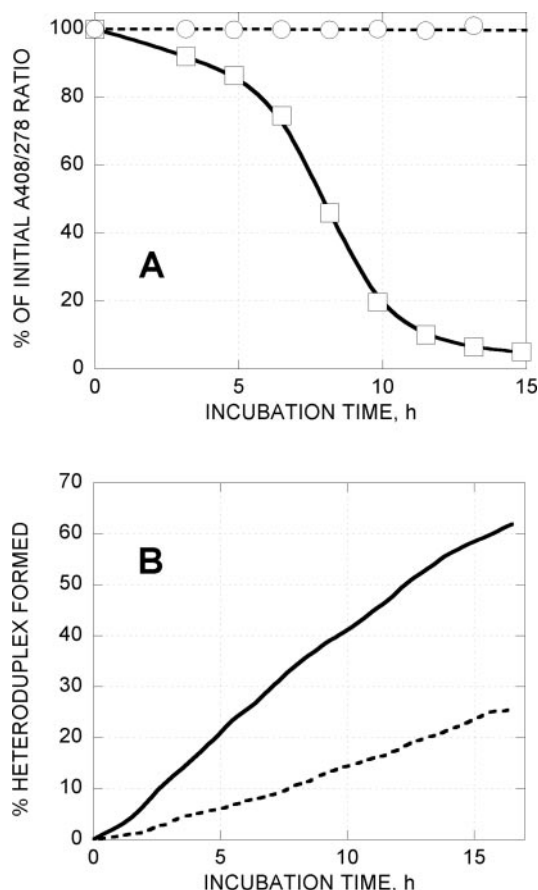


FIG. 3. Kinetic analyses of FTR-Trx interactions. A, change of the absorbency ratio during incubation of an equimolar mixture of FTR C57S and Trx *f* C49S in 20 mM triethanolamine-Cl buffer, pH 7.3, at 25 °C (squares). As a control, FTR C57S was incubated alone under the same conditions (circles). Absorbency readings at 408 and 278 nm were taken automatically at 100-min intervals. B, comparison of the rate of heteroduplex formation between WT or H86Y mutant FTR and Trx *m* C40S. 15 nmol of FTR were incubated with 20 nmol of Trx *m* C40S in 1 ml of 20 mM triethanolamine-Cl buffer, pH 7.3, at 25 °C in spectrophotometer cuvettes. The reaction mixture contained, in addition, 14 mM 2-mercaptoethanol to keep the mutant Trx monomeric. The percentage of heteroduplex formed was calculated from the change of the 408/345 nm absorbency ratio. Continuous line, FTR WT-Trx *m* C40S; broken line, FTR H86Y-Trx *m* C40S.

C87A are identical (compare in Table I). By contrast, the spectra of the heteroduplexes formed with WT or H86Y mutant FTR are comparable with the spectra of *N*-ethylmaleimide-modified FTR or mutant C57S (Fig. 1). This suggests that the redox state of the cluster is altered. The spectral change, which is most pronounced at 345 nm, provided a useful measure to follow complex formation over time as documented in Fig. 3B for the reaction with Trx *m* C40S. Similar results were obtained with Trx *f* C49S. A comparison of the kinetics between WT FTR and mutant H86Y reveals that the mutant FTR reacts more slowly.

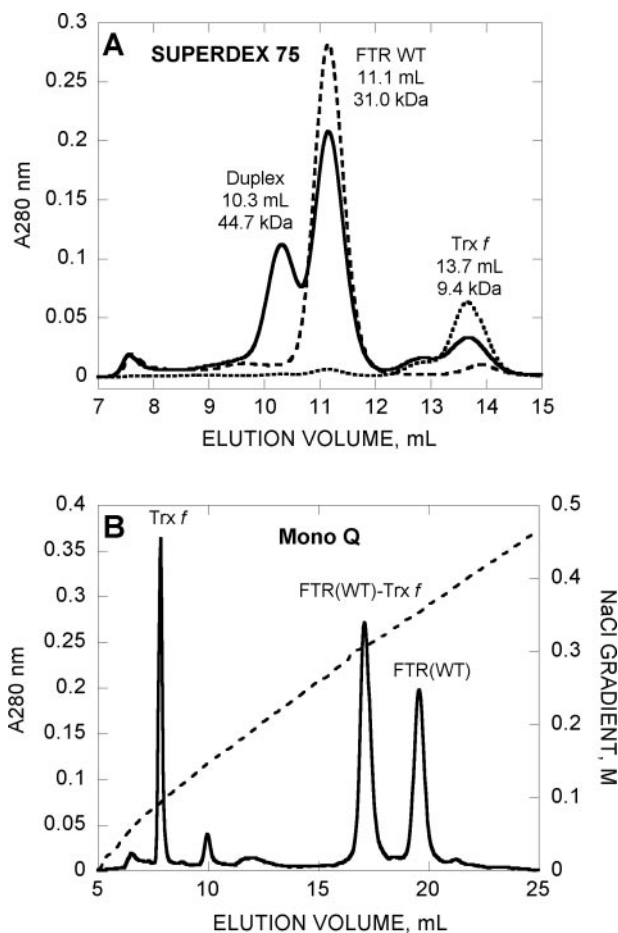


FIG. 4. Chromatographic analyses of FTR-Trx heteroduplex. *A*, analytical gel filtration by FPLC on a Superdex 75 HR 10/30 column. The samples were chromatographed Trx *f*, FTR(WT), and FTR(WT)-Trx *f* heteroduplex in a buffer containing 50 mM potassium P_i , pH 7.0, 150 mM NaCl at a flow rate of 1.0 ml/min. The elution volumes and the corresponding molecular masses calculated from calibration runs are indicated above the peaks. *B*, separation of FTR(WT)-Trx *f* heteroduplex from non-reacted proteins by ion-exchange chromatography on a FPLC Mono Q HP 5/5 column. The proteins were eluted with a gradient of 20 ml of 0–500 mM NaCl in 20 mM triethanolamine-Cl, pH 7.3, buffer.

On the Trx interaction side of the FTR, Cys-30 represents an accessible thiol. A titration of accessible thiols in the heteroduplexes by 5,5'-dithiobis(2-nitrobenzoic acid) can therefore provide some information about the coverage of this surface by Trx. In the FTR-Trx *f* complex one thiol was found; however, none was found in the complex with Trx *m*. Because Trx *f* contains an accessible Cys on its surface and Trx *m* has none (25), this result suggests that Cys-30 on the FTR surface is masked by the bonded Trx.

The heteroduplex between WT FTR and Trx represents a stable reaction intermediate with an oxidized Fe-S cluster. Its reduction should dissociate Trx from FTR, which can be shown by gel filtration. It is assumed that in the chloroplast, light-reduced ferredoxin delivers the electron necessary to reduce the Fe-S cluster and thereby breaks the disulfide bond linking the two molecules. We have therefore incubated the WT FTR-Trx heteroduplex with ferredoxin, thylakoids, and ascorbate/dichlorophenol-indophenol as electron source and observed complete dissociation in the light. However, control experiments showed that ferredoxin is not required and that even in the dark, partial dissociation is obtained. *In vitro* ferredoxin can also be reduced via FNR with an excess of NADPH + H^+ . In this reduction system both FNR and NADPH + H^+ in a 50-fold excess over the heteroduplex were needed to obtain

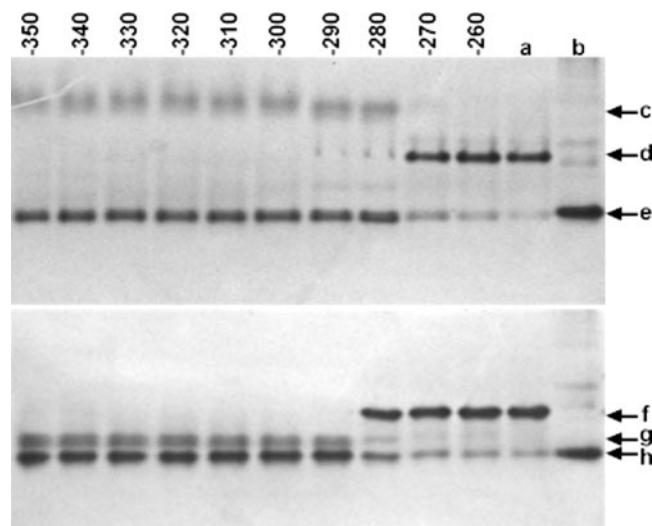


FIG. 5. Redox potential determination of FTR-Trx heteroduplexes. The heteroduplexes, at 50 μ M, were incubated under argon in 300 mM Tris-Cl, pH 7.0, containing 100 mM mixtures of oxidized and reduced DTT of defined redox potentials. After 2 h, samples corresponding to 200 pmol were separated by native gel electrophoresis on a 15% gel. *Top gel*, heteroduplex FTR-Trx *f*. *Bottom gel*, heteroduplex FTR-Trx *m*. *a*, heteroduplex control without DTT; *b*, FTR control; *c*, Trx *f*; *d*, heteroduplex FTR-Trx *f*; *e*, free FTR; *f*, heteroduplex FTR-Trx *m*; *g*, Trx *m*; *h*, free FTR. The redox potentials are given in millivolts.

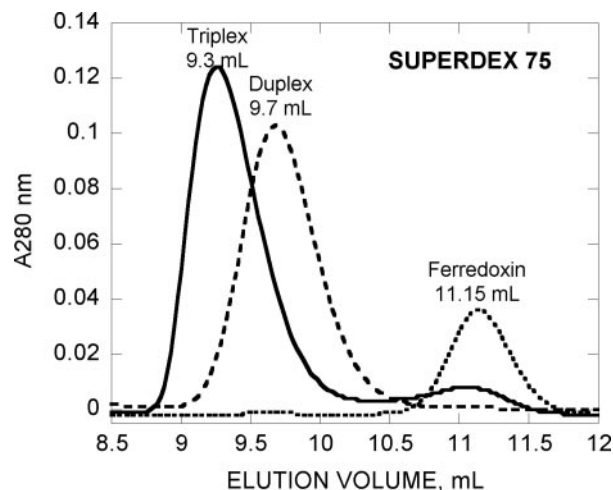
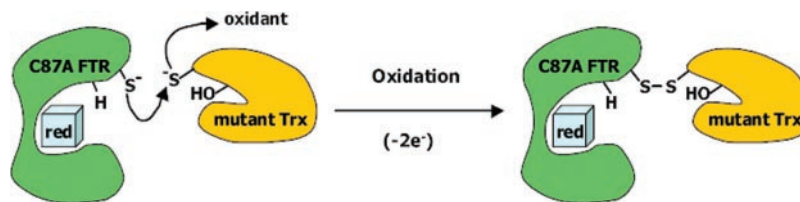


FIG. 6. Chromatographic analysis of the ferredoxin-FTR-Trx triplex. Protein mixtures were separated by gel filtration on a Superdex 75 HR 10/30 column. The samples, 1 nmol of ferredoxin-FTR(WT)-Trx *m* triplex (*Triplex*), FTR(WT)-Trx *m* heteroduplex (*Duplex*), or ferredoxin were chromatographed in a buffer containing 20 mM triethanolamine-Cl, pH 7.3, 50 mM NaCl at a flow rate of 1.0 ml/min. The elution volumes are indicated above the peaks.

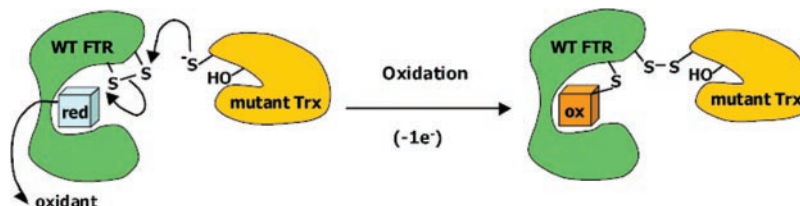
dissociation. Here again, the presence of ferredoxin was not required.

We have also compared the effect of different chemical reductants on the dissociation of the WT FTR-Trx *f* or *m* heteroduplex by gel electrophoresis and spectrophotometry. Reduced glutathione had no effect and mercaptoethanol had only a weak effect at concentrations of a 1000-fold excess over the heteroduplex. DTT, at a 200-fold excess, was more efficient, showing a dissociation kinetic with a 50-min lag phase. Dithionite was the most efficient. A 40-fold excess immediately broke the disulfide bond linking the two proteins and reestablished the spectrum of free WT FTR. When the FTR(C87A)-Trx *f* heteroduplex was similarly treated with dithionite, Trx *f* was not dissociated.

Redox Potentials of the Intermolecular Disulfide Bonds—The



SCHEME 1



SCHEME 2

above results suggest that it should be possible to estimate the redox potential of the intermolecular disulfide bridge by comparing the dissociation of the FTR-Trx heteroduplex at different ambient redox potentials. We equilibrated the heteroduplexes in incubation mixtures of known redox potentials and subsequently analyzed them by gel electrophoresis. Fig. 5 shows the results obtained with the heteroduplexes between WT FTR and Trx *f* or *m*, which indicate a potential of -270 ± 10 mV for the complex with Trx *f* and -280 ± 10 mV for the one with Trx *m*. With the FTR(C87A)-Trx *f* duplex we observed only partial dissociation down to -390 mV.

Formation of a Triple Complex among FTR, Trx, and Ferredoxin—According to the proposed reaction mechanism, the FTR should be able to interact simultaneously with Trx and ferredoxin. We therefore were looking for evidence of complex formation between the heteroduplex FTR-Trx and ferredoxin by gel filtration and spectrophotometry. When an equimolar mixture of FTR-Trx *m* heteroduplex and ferredoxin was chromatographed at low ionic strength (Fig. 6), a single peak (triplex) eluted from the column at a lower elution volume (9.3 ml) than either the heteroduplex (9.7 ml) or ferredoxin (11.16 ml). When the molar ratio in the mixture was modified to 2:1 in favor of ferredoxin, a peak of free ferredoxin appeared, and when the ratio was changed in the opposite direction, a shoulder on the profile of the triplex indicated free heteroduplex. Identical elution profiles were obtained with the FTR-Trx *f* heteroduplex. These observations are corroborated by difference spectroscopy. Both heteroduplexes were titrated with ferredoxin at 0 M NaCl, and we obtained titration curves identical to the one shown in Fig. 2A indicating a non-covalent complex between one ferredoxin and one heteroduplex molecule. These results clearly demonstrate that FTR is capable of interacting simultaneously with Trx and ferredoxin forming a 1:1:1 complex.

DISCUSSION

The FTR has structural features that are unique and enable this enzyme to reduce disulfides with electrons from a Fe-S cluster. This reduction is possible because of the close proximity and the interactions of the two important catalytic structures, the 4Fe-4S cluster and the redox-active disulfide bridge.

The structural analyses show that Cys-57, which is part of the redox-active disulfide, is close to the protein surface and should act as the attacking nucleophile in the reduction of Trx (5, 8, 9). We have replaced this Cys with a Ser residue, which leaves Cys-87, the buried partner residue of the disulfide bridge, as a free thiol. The mutant protein is no more active and has the same spectral characteristics as the *N*-ethylmaleimide-

modified FTR. This indicates that the Fe-S cluster is in its oxidized state with one of its iron atoms forming a fifth ligation to the sulfur of Cys-87. This appears to be a favorable conformation rendering the mutant by itself more stable than the WT protein. The mutant protein can be reversibly reduced with dithionite, and this is accompanied by a change of the spectrum to that of the resting WT enzyme. Thereby Cys-87 becomes reduced and switches from being a cluster ligand to a thiol or thiolate. The ferredoxin interaction surface appears to be unaltered, because the protein forms the 1:1 non-covalent complex with ferredoxin like the WT FTR. However, with Trxs no complex formation is observed, confirming that Cys-57 is part of the intermolecular disulfide and that Cys-30 on the Trx interaction surface is not involved in any covalent interaction. Surprisingly, in the presence of the mutant Trx *f* C49S, the FTR C57S loses color indicating a degradation of the Fe-S cluster. We do not know whether this is caused by the non-covalent contact of the two proteins or by some interaction between the accessible cysteines on the protein surfaces.

The partner residue of the redox-active disulfide, Cys-87, is very close to an iron atom of the cluster and apparently crucial for its stability. In the resting state of the enzyme the sulfur shows some weak interaction with this iron and becomes its fifth ligand in the one-electron-reduced intermediate (13). Replacing the sulfur by a hydroxyl in the C87S mutant perturbs this interaction and renders the cluster, and as a consequence the whole protein, unstable. This has also been observed with the spinach FTR (7). By contrast, the introduction of a hydrophobic side chain, the C87A mutation, appears to be compatible with the cluster. However, this enzyme is significantly less stable than the WT or the other mutant FTRs. This mutant shows a spectrum very similar to the resting WT FTR. The small deviation in the 408/345 absorbency ratio might be because of the missing interaction between the cluster iron and residue 87. Through its free Cys-57 this mutant FTR forms covalent heteroduplexes with Trxs.

His-86 is located between a Cys liganding the Fe-S cluster and the buried inaccessible Cys of the active site. Based on its properties and on structural considerations we proposed that it might increase the nucleophilicity of the active-site Cys-57 (8). Our present results seem to confirm this hypothesis. The H86Y mutant showed a low catalytic activity in the activation of fructose-1,6-bisphosphatase, and the kinetic of heteroduplex formation with Trx was clearly slower than with the WT FTR. The other properties of this mutant were comparable with those of the WT protein.

An interesting aspect of these studies was the formation of

protein-protein complexes among ferredoxin, FTR, and Trx. A non-covalent complex between FTR and ferredoxin has already been reported for the spinach proteins (26, 27). We observed identical high affinity 1:1 complexes between *Synechocystis* ferredoxin and WT, as well as all three mutant FTRs. These complexes were stable except for the one with the C87A mutant FTR. Here a disintegration of the cluster was observed when a 1:1 ratio of the two proteins was reached. Because the interaction between a cluster iron and the sulfur of Cys-87 is missing, the cluster is probably more labile and not able to withstand the slight deformation due to the electrostatic forces stabilizing the complex.

We have obtained stable covalent heteroduplexes between active-site mutant Trxs (Trx *f* C49S or Trx *m* C40S) and FTR, WT, or mutants H86Y and C87A but not mutant C57S. The visible absorbency spectrum of the heteroduplex with the active-site mutant C87A is indistinguishable from the spectrum of the free mutant FTR. The absence of any change suggests that the cluster stays in its 2+ redox state and that the covalent attachment of Trx *f* has no influence on the cluster. By contrast, heteroduplexes formed with either WT or H86Y FTR have visible absorbency spectra that superimpose with the spectrum of the C57S mutant or *N*-ethylmaleimide-modified FTR. This implies that the cluster has become oxidized, and the sulfur of Cys-87 has connected to an iron atom of the cluster as a fifth ligand thus stabilizing the heteroduplex.

The mechanisms of heteroduplex formation with either mutant C87A or WT FTR must be different. In the case of the mutant C87A FTR a disulfide bond is made between two thiolates with the concomitant removal of two electrons by an oxidant, which in our system is dissolved oxygen (Scheme 1). In the case of WT FTR one disulfide bond, the active-site disulfide of FTR, has to be opened before another one, between FTR and Trx, can be formed, accompanied by the removal of one electron (Scheme 2). The active-site disulfide of the FTR may be broken by the attacking Trx, helped by the cluster draining the electron. We have indications that oxidants, *e.g.* ferrocyanide, or mediators with more positive redox potentials than the FTR, *e.g.* anthraquinone 2,6-disulfonic acid, accelerate the heteroduplex formation. Further experiments are needed to better understand the mechanism of heteroduplex formation.

According to the proposed reaction mechanism for Trx reduction by FTR, the heteroduplex represents the one-electron-reduced reaction intermediate. This intermediate is thought to be dissociated by an electron provided by ferredoxin. We incubated the heteroduplexes with ferredoxin, reduced either photochemically with light and thylakoids or enzymatically with NADPH and FNR. Surprisingly, in both reduction systems the dissociation was independent of ferredoxin, *i.e.* FNR or thylakoids were capable of delivering electrons directly to the heteroduplex and releasing Trx. With the thylakoids we even observed dissociation in the dark, which, however, was increased in the light. Thylakoids appear to contain some "reductants" capable of interacting with the FTR through the Fe-S cluster or acting directly on the mixed disulfide bond. We do not know whether these ferredoxin-independent reductions occur *in vivo* or only under our *in vitro* conditions. Our experiments do not provide any kinetic information. It may well be that *in vivo* the reduction by ferredoxin is by far the most efficient and therefore the preferred mechanism.

Among the chemical reductants dithionite was the most efficient in reducing the mixed disulfide bond and dissociating Trx. This corroborates earlier reports (11) and the results obtained with mutant C57S showing that dithionite alone is capable of reducing the Fe-S cluster in analogues of the one-electron-reduced intermediate. The electrons are probably fun-

neled through the cluster to Cys-87, which becomes the attacking nucleophile. Thereby the cluster is reduced as seen by the spectral change. In the C87A mutant the reduction by dithionite is not possible because of the already reduced cluster and the absence of Cys-87, and the mixed disulfide bond cannot be broken. The reduction of the reaction intermediates or their analogues without the need of ferredoxin contrasts with the fact that the disulfide bridge of resting FTR can only be opened by reduced ferredoxin or some reduced mediators (10, 22), a difference we cannot currently explain with our results.

The redox potentials of the mixed disulfide bonds between FTR and Trxs are 40–50 mV more positive than the potential of the active-site disulfide of FTR (midpoint redox potential (E_m), pH 7.0 = –320 mV). These significantly more positive redox potentials make the second step of Trx reduction, the liberation of reduced Trx, a more favorable reaction. The heteroduplex between mutant FTR C87A and Trx *f* C49S displayed quite a different behavior. At potentials lower than –280 mV, down to –390 mV, only a partial dissociation was observed. This is probably because this mutant FTR cannot reform an active-site disulfide. Further spectroscopic studies will provide more information on the properties of the different mutant FTRs.

The heteroduplexes were able to interact with ferredoxin non-covalently, thus forming triple complexes with a 1:1:1 component ratio and confirming nicely the proposed interaction scheme (8). Titrations of the heteroduplexes with ferredoxin yielded difference spectra that were identical to those obtained with FTR alone, and the affinities were also essentially the same. These observations suggest that the FTR is not subjected to major structural changes following the binding of Trxs. Detailed information on these aspects will be provided by the structural analyses of the different protein-protein complexes.

Acknowledgments—We thank D. B. Knaff for stimulating discussions and Ophélie Rossetti, Noa Ferrari, and Anne-Lise Stritt-Etter for technical assistance in some of the experiments.

REFERENCES

- Schürmann, P., and Buchanan, B. B. (2001) in *Advances in Photosynthesis* (Aro, E.-M., and Andersson, B., eds) Vol. 11, pp. 331–361, Kluwer Academic Publishers, Dordrecht, The Netherlands
- Buchanan, B. B., Schürmann, P., Wolosiuk, R. A., and Jacquot, J.-P. (2002) *Photosynth. Res.* **273**, 215–222
- Chueca, A., Sahrawy, M., Pagano, E. A., and López Gorgé, J. (2002) *Photosynth. Res.* **74**, 235–249
- Miginiac-Maslow, M., Johansson, K., Ruelland, E., Issakidis-Bourguet, E., Schepens, I., Goyer, A., Lemaire-Chamley, M., Jacquot, J.-P., Le Maréchal, P., and Decottignies, P. (2000) *Physiol. Plant.* **110**, 322–329
- Dai, S., Schwendtmayer, C., Schürmann, P., Ramaswamy, S., and Eklund, H. (2000) *Science* **287**, 655–658
- Schwendtmayer, C., Manieri, W., Hirasawa, M., Knaff, D. B., and Schürmann, P. (1998) in *Photosynthesis: Mechanisms and Effects* (Garab, G., ed) pp 1927–1930, Kluwer Academic Publishers, Dordrecht, The Netherlands
- Manieri, W., Franchini, L., Raeber, L., Dai, S., Stritt-Etter, A.-L., and Schürmann, P. (2003) *FEBS Lett.* **549**, 167–170
- Dai, S., Schwendtmayer, C., Johansson, K., Ramaswamy, S., Schürmann, P., and Eklund, H. (2000) *Q. Rev. Biophys.* **33**, 67–108
- Chow, L.-P., Iwadata, H., Yano, K., Kamo, M., Tsugita, A., Gardet-Salvi, L., Stritt-Etter, A.-L., and Schürmann, P. (1995) *Eur. J. Biochem.* **231**, 149–156
- Staples, C. R., Gaynard, E., Stritt-Etter, A. L., Telsler, J., Hoffman, B. M., Schürmann, P., Knaff, D. B., and Johnson, M. K. (1998) *Biochemistry* **37**, 4612–4620
- Staples, C. R., Ameyibor, E., Fu, W., Gardet-Salvi, L., Stritt-Etter, A.-L., Schürmann, P., Knaff, D. B., and Johnson, M. K. (1996) *Biochemistry* **35**, 11425–11434
- Schürmann, P., and Gardet-Salvi, L. (1993) *Chimia* **47**, 245–246
- Jameson, G. N. L., Walters, E. M., Manieri, W., Schürmann, P., Johnson, M. K., and Huynh, B. H. (2003) *J. Am. Chem. Soc.* **125**, 1146–1147
- Klenk, H. P., Clayton, R. A., Tomb, J. F., White, O., Nelson, K. E., Ketchum, K. A., Dodson, R. J., Gwinn, M., Hickey, E. K., Peterson, J. D., Richardson, D. L., Kerlavage, A. R., Graham, D. E., Kyrpides, N. C., Fleischmann, R. D., Quackenbush, J., Lee, N. H., Sutton, G. G., Gill, S., Kirkness, E. F., Dougherty, B. A., McKenney, K., Adams, M. D., Loftus, B., and Venter, J. C. (1997) *Nature* **390**, 364–370
- Smith, D. R., Doucette-Stamm, L. A., Deloughery, C., Lee, H., Dubois, J., Aldredge, T., Bashirzadeh, R., Blakely, D., Cook, R., Gilbert, K., Harrison, R., Hoang, L., Keagle, P., Lumm, W., Pothier, B., Qiu, D., Spadafora, R.,

- Vicaire, R., Wang, Y., Wierzbowski, J., Gibson, R., Jiwani, N., Caruso, A., Bush, D., and Reeve, J. N. (1997) *J. Bacteriol.* **179**, 7135–7155
16. Schürmann, P. (2002) in *Methods in Enzymology* (Packer, L., and Sies, H., eds) Vol. 347, pp. 403–411, Academic Press, San Diego, CA
17. Balmer, Y., and Schürmann, P. (2001) *FEBS Lett.* **492**, 58–61
18. Wedel, N., Clausmeyer, S., Herrmann, R. G., Gardet-Salvi, L., and Schürmann, P. (1992) *Plant Mol. Biol.* **18**, 527–533
19. Manieri, W. (2002) *Mutational and Functional Studies on Proteins of the Ferredoxin/Thioredoxin Regulatory System*. Ph.D. thesis, University of Neuchâtel
20. Schürmann, P. (1995) in *Methods in Enzymology* (Packer, L., ed) Vol. 252, pp. 274–283, Academic Press, Orlando, FL
21. Habeeb, A. F. S. A. (1972) in *Methods in Enzymology* (Hirs, C. H. W., and Timasheff, S. N., eds) Vol. 25, pp. 457–464, Academic Press, New York, London
22. Schürmann, P., Stritt-Etter, A.-L., and Li, J. (1995) *Photosynth. Res.* **46**, 309–312
23. Laemmli, U. K., and Favre, M. (1973) *J. Mol. Biol.* **80**, 575–599
24. Hirasawa, M., Schürmann, P., Jacquot, J.-P., Manieri, W., Jacquot, P., Keryer, E., Hartman, F. C., and Knaff, D. B. (1999) *Biochemistry* **38**, 5200–5205
25. Capitani, G., Markovic-Housley, Z., del Val, G., Morris, M., Jansonius, J. N., and Schürmann, P. (2000) *J. Mol. Biol.* **302**, 135–154
26. Hirasawa, M., Droux, M., Gray, K. A., Boyer, J. M., Davis, D. J., Buchanan, B. B., and Knaff, D. B. (1988) *Biochim. Biophys. Acta* **935**, 1–8
27. De Pascalis, A. R., Schürmann, P., and Bosshard, H. R. (1994) *FEBS Lett.* **337**, 217–220